Silicon nanowire solar cells

L. Tsakalakos,[a] J. Balch, J. Fronheiser, and B. A. Korevaar
General Electric-Global Research Center, Niskayuna, New York 12309, USA

O. Sulima and J. Rand
GE Energy-Solar Technologies, Newark, Delaware 19702, USA

(Received 20 September 2007; accepted 13 November 2007; published online 7 December 2007)

Silicon nanowire-based solar cells on metal foil are described. The key benefits of such devices are discussed, followed by optical reflectance, current-voltage, and external quantum efficiency data for a cell design employing a thin amorphous silicon layer deposited on the nanowire array to form the *p-n* junction. A promising current density of $\sim 1.6\ \mathrm{mA/cm^2}$ for 1.8 $\mathrm{cm^2}$ cells was obtained, and a broad external quantum efficiency was measured with a maximum value of ~12% at 690 nm. The optical reflectance of the silicon nanowire solar cells is reduced by one to two orders of magnitude compared to planar cells. © *2007 American Institute of Physics*. [DOI: 10.1063/1.2821113]

In recent years, there has been a significant, resurgent interest in renewable energy systems. Solar energy conversion is of particular interest owing to the abundance of the source. The vast majority of today's commercial solar cell modules are based on crystalline Si, yet there is growing interest in thin film (so called Generation II) solar cells,[1] as well as Generation III high efficiency/low cost solar cell concepts,[2] some of which require the use of nanostructures. Nanowire (NW) based solar cells are a promising class of photovoltaic (PV) devices due to several performance and processing benefits they enable, including a direct path for charge transport afforded by the geometry of such nanostructures.

The application of nanowires (and nanorods, defined here as having an aspect ratio $\leqslant 5:1$) to solar cells has been attempted in several device configurations and materials systems. Nanowire/rod-enabled solar cells demonstrated to date have been primarily based on hybrid organic-inorganic materials or have utilized compound semiconductors such as CdSe. Huynh *et al.* utilized CdSe nanorods as the electron-conducting layer of a hole conducting polymer-matrix solar cell[3] and produced an efficiency of 1.7% for AM1.5 irradiation. Similar structures have been demonstrated for dye-sensitized solar cells using titania or ZnO nanowires, with efficiencies ranging from 0.5% to 1.5%.[4,5] These results, as well as other recent studies,[6–8] show the benefits of using nanowires for enhanced charge transport in nanostructured solar cells compared to other nanostructured architectures. Here, we present an all-inorganic, large-area solar cell concept based on Si nanowires (SiNW) with the potential to provide cells with equal or better performance to crystalline Si yet with processing methods similar to thin film solar cells.

Our own calculations, which assume conventional semiconductor physics (no quantum effects), and those of others,[9] have shown that Si nanowire-based solar cells provide an efficiency entitlement on the order of 15%–18% depending on nanowire size and quality. It is possible to form the *p-n* junction conformally about the nanowire surface in a high-density array, which has the benefit of decoupling the absorption of light from charge transport by allowing lateral diffusion of minority carriers to the *p-n* junction (which is at most 50–500 nm away) rather than many microns away as in Si bulk solar cells. Furthermore, we have shown that the optical properties of Si nanowire arrays are significantly different from those of solid thin films of the same thickness in that the optical absorption is dramatically increased across the spectrum.[10] The silicon nanowires may be synthesized using standard techniques such as chemical vapor deposition (CVD), with the possibility of direct growth on low cost (e.g., glass) and flexible substrates such as metal foil. Finally, the use of CVD grown nanowire structures may yield solar cells with an improved cost benefit compared to bulk solar cells owing to the lower materials consumption (only gases are used for fabricating the active material), yet comparable efficiency to bulk crystalline Si.

Figure 1(a) shows a schematic of the Si nanowire solar cell design and Fig. 1(b) shows typical plan-view and cross-sectional scanning electron micrographs of a Si NW solar cell fabricated on a stainless steel (SS) foil. While the focus of this work is on cells fabricated on SS substrates, we have also fabricated Si NW solar cells on degenerately doped Si substrates with a Ti/Al back contact for test purposes. Device fabrication begins with first cleaning the SS substrates using standard solvents, followed by sputter deposition of a 100-nm-thick Ta_2N film. The Ta_2N thin film[11] serves as an electrical back contact for the nanowire arrays as well as a diffusion barrier during nanowire growth. Following deposition of a 50-Å-thick Au film, catalytic CVD employing the vapor-liquid-solid (VLS) growth mechanism[12,13] is used to grow *p*-type Si nanowires (diameter=109±30 nm, length ~16 μm) with silane, hydrogen, hydrochloric acid, and trimethylboron[14] at 650 °C for 30 min. The NW array is then processed to create a dielectric isolation layer by oxidation in a dry oxygen environment at 800 °C, followed by spin coating with photoresist and partial etch back of the resist by reactive ion etching. The nanowires are then dipped in a buffered oxide etch (BOE) (6% HF in de-ionized water and buffered with ammonium fluoride) to remove the grown oxide on the exposed nanowire surfaces and the photoresist stripped using acetone.

The array is subsequently coated with a plasma-enhanced chemical vapor deposited (PECVD), conformal

[a]Author to whom correspondence should be addressed. Electronic mail: tsakalakos@research.ge.com.

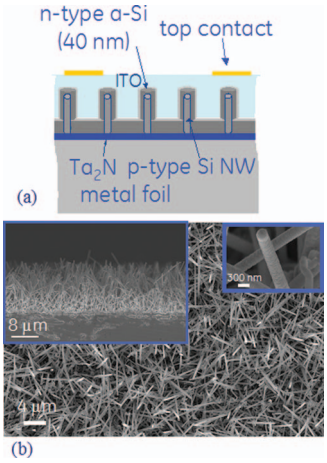

FIG. 1. (Color) Structure of the demonstrated all-inorganic silicon nanowire solar cell. (a) schematic cross-sectional view of the Si nanowire solar cell architecture. The nanowire array is coated with a conformal *a*-Si:H thin film layer. (b) Scanning electron micrograph (plan view) of a typical Si nanowire solar on stainless steel foil, including *a*-Si and ITO layers with insets showing a cross-sectional view of the device and a higher magnification of an individual Si nanowire coated with *a*-Si and ITO.

n-type amorphous silicon (*a*-Si:H) layer (40 nm) to create the photoactive *p-n* junction. This step is closely coupled (within ~30 min) to the previous BOE and photoresist removal steps, though regrowth of a very thin native oxide cannot be fully prevented. The PECVD deposition was performed in an Oxford Plasma 100 system with a total pressure of 1 Torr, a temperature of 180 °C, and the following gases: SiH_4:H_2:Ar:PH_3 in the ratios of 1:2.5:7.5:0.125.

Conformal PECVD *a*-Si:H thin films allow for a low temperature, scaleable means of creating a *p-n* junction to the Si NW arrays. Furthermore, the good passivating properties of *n*-type *a*-Si:H films are well known.[15] While the minority carrier lifetimeand surface recombination velocity in ouor nanowires is generally unknown, we expect that the presence of the *a*-Si film on the nanowires will be helpful in minimizing nonradiative surface recombination. It is also possible to deposit a nanocrystalline Si (nc-Si:H) *n* or *i-n* layer, though nc-Si:H is generally not as effective in passivating crystalline Si.[16]

After *a*-Si:H deposition, the array is sputter coated with a 200-nm-thick transparent conducting indium tin oxide (ITO) layer to electrically tie all the wires together. Top finger contacts were created by shadow evaporation of Ti (50 nm)/Al (2000 nm). The SS substrate was then spin coated with photoresist and diced into 1×1 or 1.2×1.5 cm pieces, after which the photoresist was removed in acetone. The solar cells were then mounted (using silver epoxy) onto a Cu-coated printed circuit board with a notch and a thin Au wire was manually attached to the top finger contact. Testing was performed in a Thermo-Oriel solar simulator setup (AM1.5) calibrated with a Si solar cell from the National Renewable Energy Laboratory (NREL).

As noted above, we expect the Si NW PV devices to show improved optical characteristics compared to planar devices. The optical reflectance (specular) of a typical Si NW cell compared to a planar device is shown in Fig. 2, along with a picture of two representative devices. The Si NW cells show a reduction in reflectance of one to two orders of magnitude over the full spectrum ranging from 300 to 1100 nm. We note that no additional antireflective layer was employed

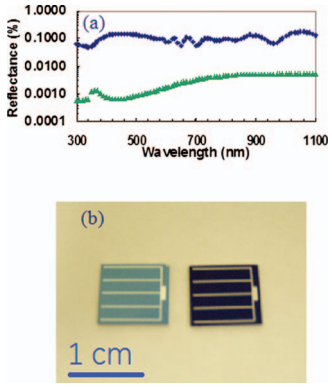

FIG. 2. (Color) Optical characteristics of Si nanowire solar cells. (a) Specular reflectance (log scale) for a nanowire cell (green) compared to a thin film *p-i-n* *a*-Si solar cell (blue) showing a significantly reduced reflectance (<1%) for the nanowire cell. (b) Picture of a planar *a*-Si:H solar cell fabricated on a degenerately doped Si substrate (left) and a Si NW solar cell fabricated on the same type of substrate with a 1 cm^2 area. The Si NW solar cell has a dark, matte appearance compared to the planar device. No antireflective thin film layers were applied to either cell.

in either the nanowire or planar samples. Visually, the NW devices have a matte finish and are significantly darker in appearance compared to the planar cells [Fig. 2(b)].

Figure 3(a) shows the typical dark and light (under AM1.5 equivalent conditions) current-voltage curves of such a Si NW solar cell. Clear rectifying behavior and power generation is observed in these 1.8 cm^2 devices with a 3 mA photocurrent. The open circuit voltage of the best devices was ~130 mV, which is slightly smaller than that of the single nanowire devices demonstrated by Tian *et al.*,[7] and the fill factor was ~0.28. Both high series and low shunt resistances appear to limit the efficiency of the devices. Figure 2(b) shows the quantum efficiency (Optronics Laboratories, Inc.) of a typical nanowire solar cell sample deposited on SS foil. While, at present, the conversion efficiency of these cells is low (~0.1%), the nanowire cells on SS foil showed a spectrally broad external quantum efficiency (EQE), demonstrating that the observed photovoltaic effect is due to absorption within the nanowire array. Our previous optical studies have shown that the effective absorption within the nanowire array shows a similar shape to the observed EQE curve in the near-IR range,[10] though at shorter wavelengths

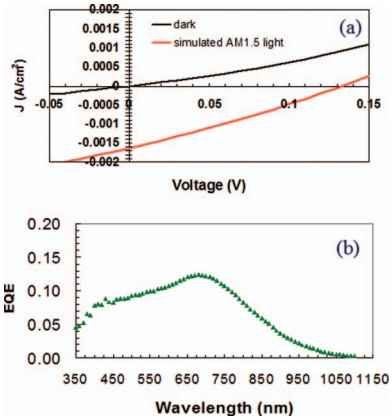

FIG. 3. (Color) Optoelectronic characteristics of typical Si nanowire solar cell devices fabricated on SS steel substrates. (a) Dark and light (under simulated AM1.5 conditions) current-voltage characteristics of a typical Si nanowire solar cell, as shown in Figure 1. (b) Measured external quantum efficiency (EQE) for a silicon nanowire cell showing a broad EQE response.

(below ~650 nm) we observe a reduction in the EQE of the devices. This is most likely related to loss of high energy light by absorption in the unoptimized, relatively thick *a*-Si:H film and/or losses within the ITO layer, though this point requires further study. The peak EQE measured is ~12% at 690 nm.

There are several features of these devices that impact PV performance. Of particular importance is the geometry of the nanowires. While the nanowire length employed in these samples is sufficient (~16 μm),[9] the mean nanowire radius should be optimized such that it is approximately equal to the mean minority carrier diffusion length in the nanowires. The depletion region in the nanowires must be kept small so that the nanowires are not fully depleted. A relatively large quasineutral core region is, thus, desired to channel holes down to the back contact. To this end, the doping level in both the nanowires (estimated to be $\sim 10^{18}$ cm^{-3} based on single nanowire transistor and secondary ion mass spectroscopy measurements performed in our laboratory) and in the *a*-Si:H layer have been targeted to be approximately equal, yielding an expected depletion width of ~50 nm. However, we believe this unoptimized diameter distribution provides a partial explanation of why V_{oc} is low in these devices, as does the fact that there may be regions of local shunting across the cells. Additionally, the use of Au as a catalyst particle for nanowire growth, which is well known to limit lifetime in Si,[17,18] must ultimately be replaced with another metal.

Another potential factor impacting performance is the presence of the Ta_2N back contact, which may provide a source of Ta diffusion into the Si nanowires and, thus, reduce minority carrier lifetime. However, based on structural[19] and solid-state reaction considerations,[20] we do not expect a significant amount of Ta to be present in the photoactive portion of the nanowires.

In summary, we have demonstrated all-inorganic, large area, *p-n* junction silicon nanowire-based solar cells fabricated by chemical vapor deposition on stainless steel substrates. These solar cells have an efficiency entitlement comparable to typical bulk Si solar cells, yet with potential for lower cost. The processes employed to fabricate these devices are readily scalable, making this solar cell architecture a promising candidate for future photovoltaic applications. Ongoing research is focused on improving the power conversion efficiency of the cells by reducing contact resistance, minimizing shunts, optimizing nanowire geometry, and improving the *p-n* junction quality.

The authors wish to thank M. Idelchik, M. L. Blohm, E. Butterfield, D. Merfeld, T. Feist, G. Trant, C. Korman, M. Beck, C. Lavan, R. Rodrigues, R. Wortman, V. Smentkowski, and R. R. Corderman for support and helpful discussions.

[1] A. Shah, P. Torres, R. Tscharner, N. Wyrsch, and H. Keppner, Science **285**, 692 (1999).
[2] M. A. Green, Proceedings of the Fourth World Conference Photovoltaic Energy Conversion 2006, Vol. 1, p. 15.
[3] W. U. Huynh, J. J. Dittmer, and A. P. Alivisatos, Science **295**, 2425 (2002).
[4] M. Law, L. E. Greene, J. C. Johnson, R. Saykally, and P. Yang, Nat. Mater. **4**, 455 (2005).
[5] J. B. Baxter and E. S. Aydil, Appl. Phys. Lett. **86**, 053114 (2005).
[6] I. Gur, N. A. Fromer, M. L. Geier, and A. P. Alivisatos, Science **310**, 462 (2005).
[7] B. Tian, X. Zheng, T. J. Kempa, Y. Fang, N. Yu, G. Yu, J. Huang, and C. M. Lieber, Nature (London) **449**, 885 (2007).
[8] G. Andrä, M. Pietsch, T. Stelzner, F. Falk, E. Ose, S. H. Christiansen, A. Scheffel, and S. Grimm, presented at the 22nd European Photovoltaic Solar Enerergy Conference Exhibit, Milano, 3–7 September 2007 (unpublished).
[9] B. M. Kayes, N. S. Lewis, and H. A. Atwater, J. Appl. Phys. **97**, 114302 (2005).
[10] L. Tsakalakos, J. Balch, J. Fronheiser, M.-Y. Shih, S. F. LeBoeuf, M. Pietrzykowski, P. J. Codella, B. A. Korevaar, O. Sulima, J. Rand, A. D. Kumar, and U. Rapol, J. Nanophotonics **1**, 013552 (2007).
[11] H. B. Nie, S. Y. Xu, S. J. Wang, L. P. You, Z. Yang, C. K. Ong, J. Li, and T. Y. F. Liew, Appl. Phys. A: Mater. Sci. Process. **73**, 229 (2001).
[12] R. S. Wagner and W. C. Ellis, Appl. Phys. Lett. **4**, 89 (1964).
[13] Y. Cui, L. J. Lauhon, M. S. Gudiksen, J. Wang, and C. M. Lieber, Appl. Phys. Lett. **78**, 2214 (2001).
[14] K. K. Lew, L. Pan, T. E. Bogart, S. M. Dilts, E. C. Dickey, J. M. Redwing, Y. Wang, M. Cabassi, T. S. Mayer, and S. W. Novak, Appl. Phys. Lett. **85**, 3101 (2004).
[15] M. Taguchi, K. Kawamoto, S. Tsuge, T. Baba, H. Sakata, M. Morizane, K. Uchihashi, N. Nakamura, S. Kiyama, and O. Oota, Prog. Photovoltaics **8**, 503 (2000).
[16] C. Voz, I. Martin, A. Orpella, J. Puigdollers, M. Vetter, R. Alcubilla, D. Soler, M. Fonrodona, J. Bertomeu, and J. Andreu, Thin Solid Films **430**, 270 (2003).
[17] G. Bemski, Phys. Rev. **111**, 1515 (1958).
[18] W. Schmid and J. Reiner, J. Appl. Phys. **53**, 6250 (1982).
[19] N. D. Cuong, N. M. Phuong, D. J. Kim, B. D. Kang, C. S. Kim, and S. G. Yoon, J. Vac. Sci. Technol. B **24**, 682 (2006).
[20] H. Ono, T. Nakano, and T. Ohta, Appl. Phys. Lett. **64**, 1511 (1994).